

# Strength and Durability Performance of Ultra-High-Performance Cementitious Composite Enhanced with Carbon Nanofibres

J.L.G. Lim, S.N. Raman, M.F.M. Zain and R. Hamid

Faculty of Engineering and Built Environment, Universiti Kebangsaan Malaysia, Selangor, Malaysia

F.C. Lai

Hume Concrete Products Research Centre (HPFRC), Bangunan PanGlobal, Selangor, Malaysia

## ABSTRACT

*Ultra-high-performance concrete (UHPC) is known for exhibiting excellent strength and a more durable matrix compared to conventional concrete. Typically UHPC consists of carefully selected constituent materials of: ultrafine graded sand, silica fume (or other alternative binders), steel micro-fibres, and ordinary (or special blends) Portland cement. This study was initiated to synthesize a new blend of Ultra-high-performance cementitious composite (UHPCC) with compressive strength higher than 150 MPa under normal curing conditions, and to investigate the influence of two different sources of carbon nanofibres (CNF) on its strength, durability and microstructure properties. Several mix designs with different CNF percentages were designed, optimised and analysed to obtain the optimal proportion for the UHPCC, and their strength development were monitored up to 28 days. Subsequently, the durability performance of the selected UHPCC mixes were characterised through the rapid chloride permeability, Mercury Intrusion Porosimetry and water penetration tests. It was found that a stable dispersion with low CNF percentage (0.06%wt) was able to improve the water penetration, lower the rapid chloride permeability and reduced the pore sizes of the UHPCC matrix. The overall findings of the research assert that a stable dispersion of CNF contributes in positive effect on the strength and durability characteristics of UHPCC, and is feasible to enhance overall microstructure and contribute to a denser matrix. This study is part of the larger research programme to synthesize an innovative UHPCC mix for specialised applications for structures under impulsive loadings.*

**Keywords:** Carbon nanofibres (CNF); Ultra-High-Performance Cementitious Composites (UHPCC); Nano-engineered; Porosity; Durability; Compressive Strength

## 1.0 INTRODUCTION

Ultra-High-Performance Concrete (UHPC) is a type of special purpose cementitious composite developed to realize the need for impressive megastructures and extreme construction. UHPC usually exhibits ultra-high-strength properties with characteristic compressive strength of 150 MPa or higher at 28 days, and is typically produced using low water-to-binder ratio with high volume of cement and/or supplementary cementitious materials, various grading and types of fine aggregates, fibre reinforcements and chemical admixtures (Raman, 2012; Wille and Naaman, 2011). The UHPC system eliminates all the coarser particles used in the typical normal-strength concrete mix. Instead, its matrix is packed with micro-scaled materials such as silica fume and ultra-fine sand.

Due to the brittle nature of concrete, high volume of metallic fibre reinforcing system is important to provide the required ductility and delaying crack propagation (Graybeal and Davis, 2008). The

practice of incorporating discrete fibres into cementitious composites is driven by the need to overcome limitations of reduced ductility and increased brittleness in the material when it is driven to achieve higher strengths, such as in Ultra High-Performance Cementitious Composites (UHPCC). Ductal is one of the most common UHPC product, with applications in bridges, water dam and special construction, achieving compressive strength higher than 180 MPa under steam curing at 90°C. Further, it consists of 8 different constituents in its mix design (Acker and Behloul, 2004).

Carbon nanotubes/carbon nanofibres (CNT/CNF) is a potential candidate to further enhance the nano-matrix packing and characteristics of cementitious composites due to their nano-dimensional nature and good coverage in the concrete matrix (Lim *et al.*, 2018). CNT has also been reported to facilitate the enhancement in the mechanical properties and nano-filling characteristics of concrete (Metaxa *et al.*, 2012). The present study was undertaken to investigate the potential of utilising carbon nanofibres

(CNF), and their influence on the dynamic mechanical, fracture, and durability characteristics of UHPCC, designed to achieve a compressive strength of 150 MPa and higher at 28 days, under normal curing conditions. The UHPCC produced is targeted to be applied for structures subjected to high impulsive loadings, such as those subjected to blast and impact. This paper discusses on the strength and durability performance of the UHPCC mixes incorporating two types of CNF.

## 2.0 MATERIALS AND METHODS

### 2.1 Materials and Mix Design

The mix design was formulated based on a recent work by the authors (Lim *et al.*, 2015), as shown in Table 1. The first step in the experimental work was to analyse the synthesis of CNF which were obtained from two different sources, CNF-A and CNF-B. The properties of these CNFs are shown in Table 2. CNF-A and CNF-B were prepared by using different dispersion techniques, as discussed in Table 3. It was observed that CNF-A with added surfactant was stable under ultrasonication dispersion method. Meanwhile, CNF-B was observed to be stable under ultrasonication dispersion method without the addition of surfactant. Figure 1 shows the types of CNF that were produced in this study with different dispersion methods.

The optimised particle packing approach was used in designing the UHPCC mixes by adopting the following Fuller's equation, as shown in Eq. 1:

$$P(D) = \left(\frac{d}{D}\right)^q \quad (1)$$

where  $P$  is the fraction passing the sieve with opening  $D$ ,  $d$  is the particle size and  $D$  is maximum particle size of the mix. The parameter  $q$  has a value between 0 and 1. The theoretical curve by Fuller can be obtained when the value of  $q = 0.5$ , whereas the modified version by Andreasen and Andersen can be obtained when the value of  $q = 0.37$  (Brouwers and Radix, 2005). The cement and graded sand that were used in this study were sieved and passed through mesh No. 50 (approximately 0.3 mm). In enhancing the mix designs, the optimised grading curve of cement and graded sand were computed to determine the optimised grading of the modified

Andreasen's curve as presented in Fig. 2. Optimum grading of the blend will contribute to a denser matrix of the mix.

### 2.2 Specimen Preparation and Testing

To produce the UHPCC mixes, cement and graded sand were blended in a Hobart N50 planetary mixer for 3 minutes. Water and superplasticizer were added and mixed for 5 minutes until the mix became flowable. The flow value was measured in accordance with ASTM C230 within 30 seconds to ensure the workability. The fresh mix was then cast into 50 mm cube moulds for compressive strength determination, 150mm cube moulds for water penetration depth test, 50 mmH × 100 mmD cylinder moulds for rapid chloride permeability test (RCPT). All the specimens were covered with plastic sheets to prevent evaporation of water during initial curing. The specimens were demoulded after 24 h and were then cured in water at room temperature for strength and durability characterisation.

The compressive strength of specimens was determined on the 3<sup>rd</sup>, 7<sup>th</sup> and 28<sup>th</sup> day in accordance with ASTM C109. Meanwhile, 28-days specimens were used to perform all the durability tests.

The RCPT was performed in accordance to ASTM C1202. This test measures the current passing through cement-based materials in 6 h, giving an indication of the concrete resistance to chloride ion permeability. The concrete specimen used for this test was 100 mm diameter by 50 mm thick specimen. A direct current voltage of  $60 \pm 0.1$  V was applied across the two faces of the specimen and the current passing through the specimen was monitored at 30 minute intervals over a period of 6 h. The total charge passed through, in Coulombs (C) was determined.

A Micromeritics AutoPore IV 9500 apparatus was used for the Mercury Intrusion Porosimetry (MIP) test and the maximum pressure that could be applied is 210 MPa (30,500 psi), which corresponds approximately to a minimum detectable pore diameter of 6 nm. Meanwhile, the water penetration depth test was carried out in accordance to BS EN 12390:8. The 150 mm cube specimen was placed in the apparatus and a water pressure of  $500 \pm 50$  kPa was applied for  $72 \pm 2$  hrs.

**Table 1.** UHPCC mix proportions (Ratio by Mass)

| Constituents | UHPCC | UHPCC-CNF A1 | UHPCC-CNF A2 | UHPCC-CNF A3 | UHPCC-CNF A4 | UHPCC-CNF B1 | UHPCC-CNF B2 | UHPCC-CNF B3 | UHPCC-CNF B4 |
|--------------|-------|--------------|--------------|--------------|--------------|--------------|--------------|--------------|--------------|
| Cement       | 1     | 1            | 1            | 1            | 1            | 1            | 1            | 1            | 1            |
| Graded Sand  | 0.45  | 0.45         | 0.45         | 0.45         | 0.45         | 0.45         | 0.45         | 0.45         | 0.45         |
| Water        | 0.20  | 0.20         | 0.20         | 0.20         | 0.20         | 0.20         | 0.20         | 0.20         | 0.20         |
| SP           | 0.009 | 0.010        | 0.010        | 0.011        | 0.012        | 0.010        | 0.010        | 0.010        | 0.011        |
| CNF          | –     | 0.0002       | 0.0004       | 0.0006       | 0.0008       | 0.0002       | 0.0004       | 0.0006       | 0.0008       |

Scanning Electron Microscope (SEM) was used to study the microstructural characteristics of the UHPCC matrix produced in this study, at the ages above 28 days.

**Table 2.** Properties of carbon nanofibers

| Properties               | CNF-A | CNF-B   |
|--------------------------|-------|---------|
| Purity (%)               | >99   | >90     |
| Diameter (nm)            | ~40   | 30-300  |
| Length ( $\mu\text{m}$ ) | ~10   | 10-20   |
| Surface area             | >180  | 120-140 |
| Zeta Potential           | -10   | >30     |

**Table 3.** Dispersion method of carbon nanofibers

| No. | Source | Method                       | Observation    |
|-----|--------|------------------------------|----------------|
| 1   | CNF-A  | Ultrasonication              | Non-homogenous |
| 2   | CNF-A  | Ultrasonication+ surfactant* | Homogeneous    |
| 3   | CNF-B  | Ultrasonication              | Homogeneous    |

\*Polycarboxylate ether (PCE) based superplasticizer (SP)

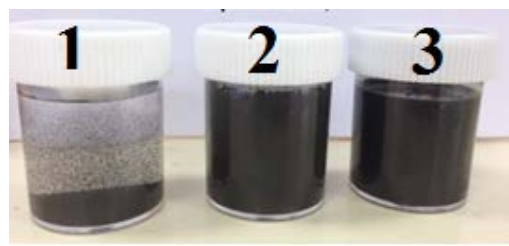


**Fig. 1.** Types of CNF suspensions

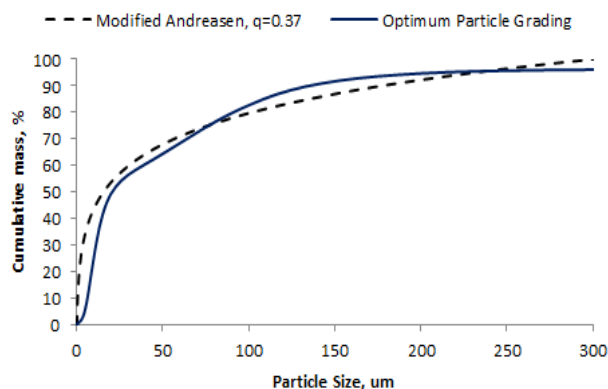


**Fig. 2.** Optimum particle packing grading

## 3.0 RESULTS AND DISCUSSION

### 3.1 Compressive Strength

Preliminary findings by the authors indicated that UHPCC with water-cement ratio of 0.20 achieved the highest 28 days compressive strength (Lim *et al.*, 2015). Hence, this mix design was further enhanced with four different percentages of CNF. CNF-A and

CNF-B help in the early age strength development at 3-days. It can be observed from the results (Fig. 3) that UHPCC made of CNF-A3 with a higher dosage of CNF (0.06%) recorded the lowest compressive strength of 115 MPa at 7 days and 140 MPa at 28 days. This may be caused by the poor dispersion and instability of the CNF sample used in the mix. UHPCC with higher CNF dosage, CNF-B3 (with 0.06% CNF-B) recorded the highest compressive strength of 140MPa and 160MPa at 7-days and 28-days, respectively. When the CNF percentage was increased, the superplasticizer dosage also needs to be increased to maintain the flowability of the fresh paste.

Microstructural analysis is essential to understand the presence and contribution of CNF in the UHPCC matrix. The presence of CNF provides better bridging in the matrix, as shown in Figures 4 and 5. It can be observed from Figure 4 that CNF-A likely “agglomerated” in the matrix. Poor dispersion of CNF-A will greatly affect the microstructure of the matrix and lower the compressive strength. Meanwhile, the more stable and good dispersion of CNF-B within the matrix will make significant contribution to the strength improvement.

Figure 4 and 5 also indicate the variation in the characteristics of CNF-A and CNF-B, i.e. being formed with different dimensional grading. CNF-A consisted of generally uniform nano-diametered tubular fibres of about 40 nm, while CNF-B was formed with a wider range of 30-300 nm diametered tubular fibres. The SEM analysis also illustrated the good bridging characteristics between CNF-B and the UHPCC matrix, whereas CNF-A agglomerated within the matrix and this may contribute in ineffective bridging with the surrounding matrix, as discussed by Siddique and Mehta (2014).

### 3.2 Durability of UHPCC

The UHPCC mix which performed the best in terms of compressive strength, UHPCC-CNF-B3, together with UHPCC-CNF-A3 mix and the control UHPCC mix, was selected for further durability analysis in the next stage. UHPCC-CNF-A3 mix was selected as it contained similar CNF percentage (0.06%) with the UHPCC-CNF-B3 mix.

#### Rapid Chloride Permeability Test (RCPT)

The dispersion of CNF-A and CNF-B did not show significant variation in terms of chloride permeability. All the UHPCC mixes produced in this study had “very low” penetrability (Fig. 6) according to ASTM C1202 classification, as their passing charges were below 1000 coulombs. The RCPT findings indicated that both UHPCC-CNF A3 and UHPCC-CNF B3 achieved lower coulombs compared to the control specimen (Fig. 6). Specimen with a dense pore structure will result in lower permeability in the RCPT (Ghazy *et al.*

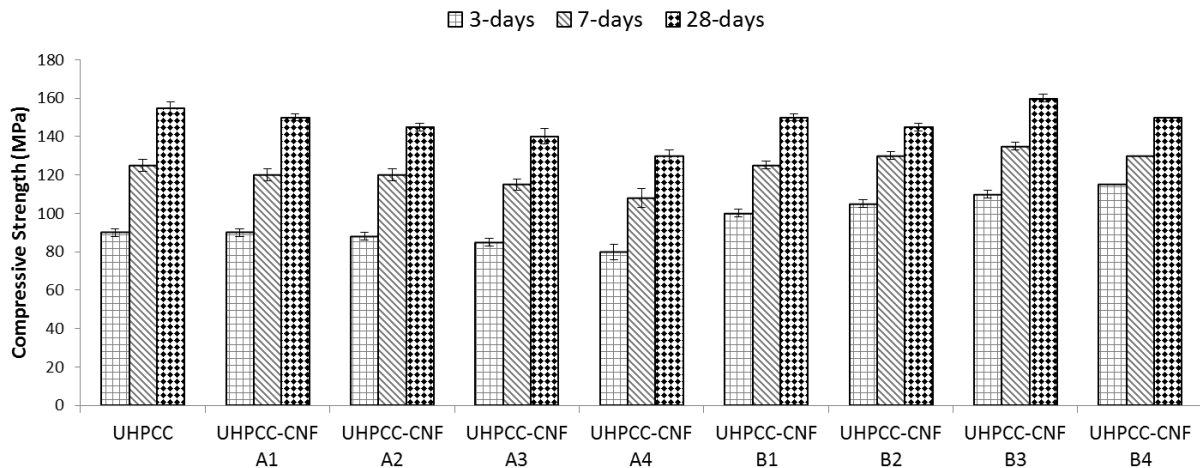


**Fig. 3.** The strength performance of UHPCC mixes

2016). The findings of RCPT has its limitations, where the classification scale can be deemed as too wide, considering that it is a measure of ion charge passed over 6 hours. Similarly, researchers have also stated on such limitations of RCPT, i.e. it is a measure of ion movement, and may not be the actual permeability depth (Dhanya and Santhanam, 2017).

structure, which eliminated all the macropores and resulted in a more durable and “water resistant” UHPCC. Figures 4 and 5 also indicated that CNF-A and CNF-B were able to fill some of the nano-pores within the UHPCC matrix.

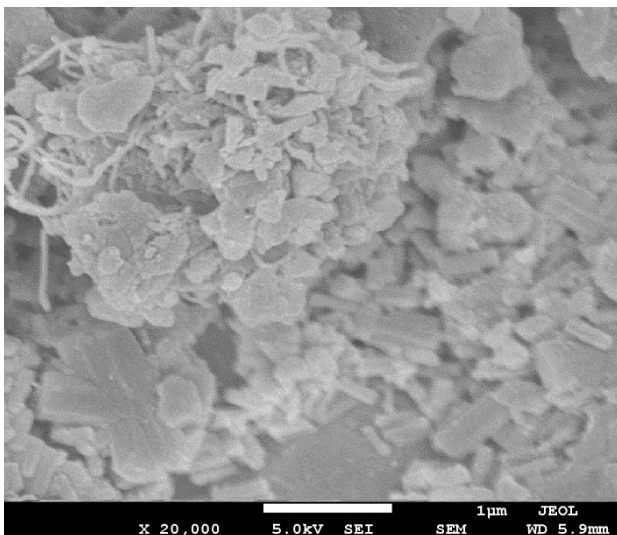


**Fig. 4.** Micrograph of CNF-A in within the UHPCC matrix

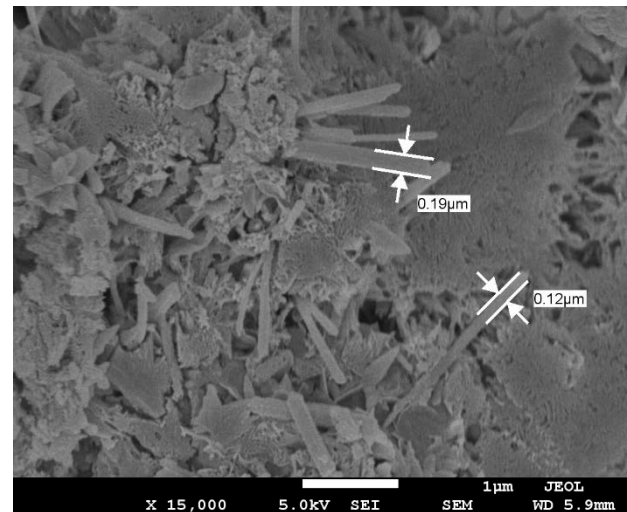


**Fig. 5.** Micrograph of CNF-B in within the UHPCC matrix

Water Penetration Depth

Figure 7 shows the water penetration depth findings, where it can be observed that both UHPCC-CNF A3 and UHPCC-CNF B3 exhibited a much reduced water penetration compared to the control specimen. The water penetration depth in UHPCC-CNF B3 and UHPCC-CNF A3 mixes were reduced by 60% and 33%, respectively, in comparison to the control. It can be deduced that the addition of 0.06% CNF was able to make the UHPCC matrix denser. However, the UHPCC-CNF B3 performed better than UHPCC-CNF A3, due to possible the agglomeration of CNF-A within the matrix, as shown in Fig. 4. Thus, UHPCC-CNF B3 exhibited a much denser microstructure compared to UHPCC-CNF A3, with smaller pore

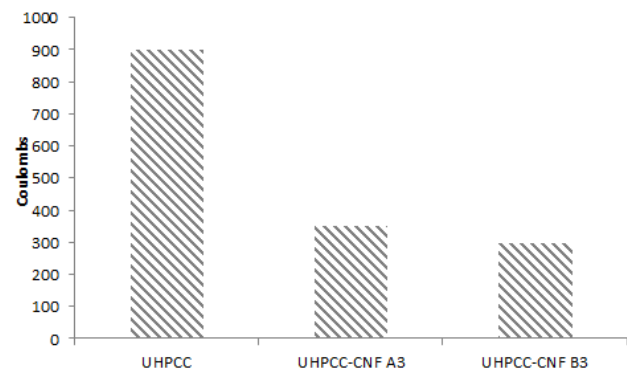


**Fig. 6.** RCPT findings of different UHPCC mixes

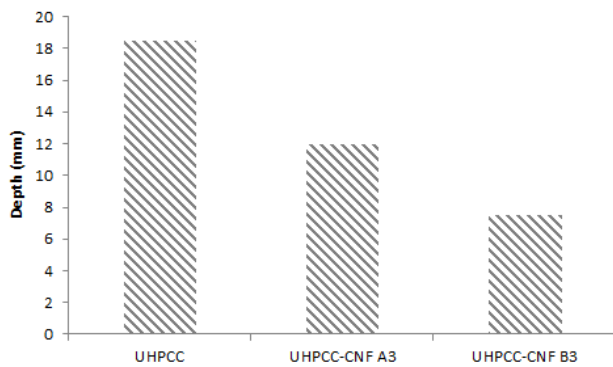


**Fig. 7.** Water penetration depth of UHPCC mixes

#### Porosity

According to Mindess *et al.* (2003), it can be observed that there is a wide range of pore sizes, from 10  $\mu\text{m}$  to less than 0.0005  $\mu\text{m}$  (0.5 nm) in diameter within the matrix of cementitious composites. The pore structure of the control UHPCC mix, and the CNF enhanced UHPCC-CNF A3 and UHPCC-CNF B3 mixes, were characterised by using the MIP technique. The findings, as shown in Fig. 8 indicates that both specimens which were enhanced with CNF experienced a much lower pore size compared to the control UHPCC mix. The additional of CNF into the matrix will be able to fill the nano-pores of the matrix (Siddique and Mehta, 2014). CNF-B with a much stable dispersion exhibited a much lower volume of pores compared to CNF-A.

Capillary pores and large capillaries (macropores) of greater than 100 nm seemed to control UHPCC specimens, and similarly pores greater than 50 nm for the UHPCC-CNF A3 specimen. UHPCC-CNF B3 only contained mesopores which were lower than 50 nm due to the stable dispersion of CNF, and the nano-pores were well connected by the CNF. This indicated that the matrix of UHPCC-CNF B3 mix was “constructed” of a much denser microstructure which eliminated the bulk water within the matrix. The capillary pores are the remnants of water-filled space

that exist between the partially hydrated cement grains which caused by macropores that can affect the transport properties of cement materials (with macropores diameter from 50 to 10,000 nm) (Mindess *et al.*, 2003). The dispersion of CNF will affect the overall microstructure of UHPCC. Figure 9 shows that there exist internal micro-voids within the cross-section of UHPCC-CNF A, while Figure 10 shows a very dense microstructure without any micro-voids in UHPCC-CNF B matrix. This observation justified the findings indicated shown in Figures 4 and 5. As discussed by Diamond (2000) there may be air voids present in pastes unless they are vacuum mixed and are intruded after the threshold pressure is reached, and these are not generally recognised as such in MIP porosity.

## 4.0 CONCLUSIONS

This study proposed a simpler version of UHPCC mix with fewer ingredients of UHPCC mix design to incorporate CNF, to achieve compressive strength of higher than 150 MPa, under normal curing conditions, and discussed the effect of CNF on the strength and durability properties of the UHPCC. The conclusions of the study are as following:

- UHPCC with 0.06% CNF-B (UHPCC-CNF B3) recorded the highest 28<sup>th</sup> day compressive strength of 160 MPa, among all the UHPCC types produced in this study.
- In general, CNF-B performed better than CNF-A due to its stable dispersion within the matrix. The stable dispersion of CNF is essential to achieve optimum strength and durability properties.
- The MIP findings showed that CNF-B improved the pore structure and resulted in a much denser matrix and better durability performance. A much denser UHPCC-CNF B3 also resulted in enhancement in terms of reduced water and chloride penetration.

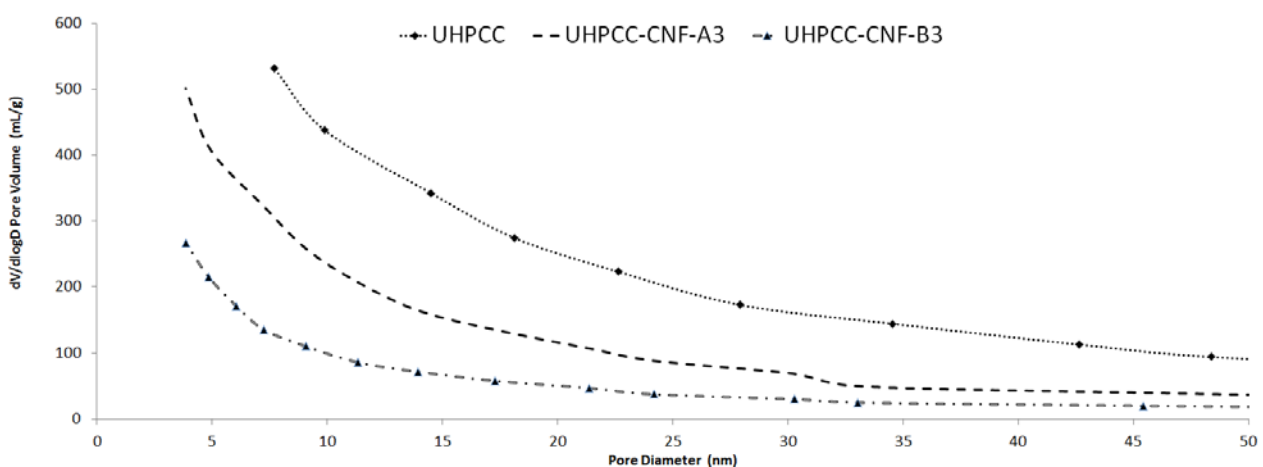


**Fig. 8.** Pore size distribution of UHPCC measured

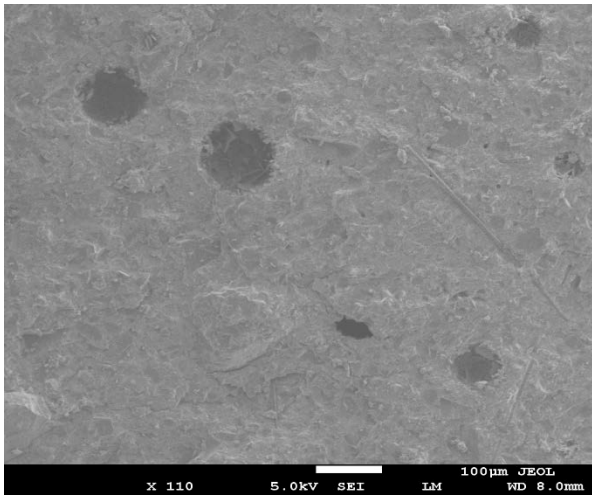


**Fig. 9.** Microstructure of UHPCC-CNF A

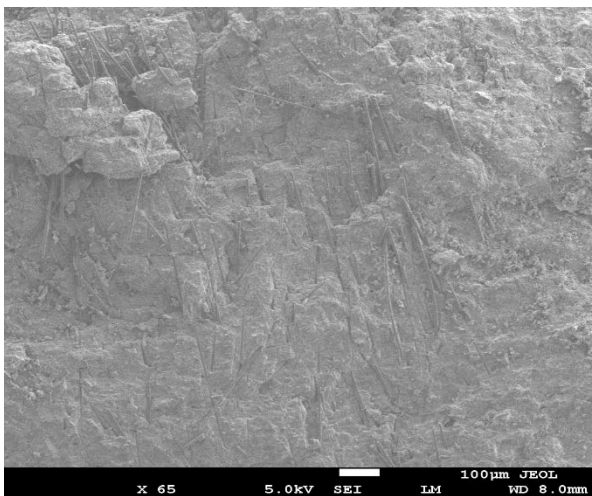


**Fig. 10.** Microstructure of UHPCC-CNF B

### Acknowledgement

This study was supported by the Fundamental Research Grant Scheme (FRGS/1/2015/TK01/UKM/02/1), awarded by the Ministry of Higher Education, Malaysia and Universiti Kebangsaan Malaysia. The authors also acknowledge ceEntek Pte. Ltd., Singapore, for supplying some of the CNF samples that were used in this study.

### References

Acker, P., Behloul, M., 2004. Ductal® Technology: A Large Spectrum of Properties, A Wide Range of Applications. Proceedings of the International Symposium on Ultra-High Performance Concrete, Kassel, Germany. pp. 11-23

ASTM, 2013. Standard Specification for Flow Table for Use in Tests of Hydraulic Cement. ASTM C230/C230M-13.

ASTM, 2011. Standard Test Method for Compressive Strength of Hydraulic Cement Mortars (Using 2-in or [50-mm] Cube Specimens). ASTM C109/C109M.

ASTM, 2000. Electrical indication of concrete's ability to resist chloride ion penetration. ASTM C1202.

Brouwers, H.J.H., Radix, H.J., 2005. Self-Compacting Concrete: Theoretical and experimental study. *Cement and Concrete Research*, 35(11): 2116–2136.

BSI, 2009. Testing hardened concrete. Depth of penetration of water under pressure. BS EN 12390-8:2009.

Dhanya, B.S., Santhanam, M., 2017. Performance evaluation of rapid chloride permeability test in concretes with supplementary cementitious materials. *Materials and Structures*, 50(1): 67.

Diamond, S., 2000. Mercury porosimetry: an inappropriate method for the measurement of pore size distributions in cement-based material. *Cement and Concrete Research*, 30(10): 1517–1525

Ghazy, A., Bassuoni, M. T., Shalaby, A., 2016. Nano-Modified Fly Ash Concrete: A Repair Option for Concrete Pavements. *ACI Materials Journal*, 113(2): 231-242

Graybeal, B., Davis, M., 2008. Cylinder or cube: strength testing of 80 to 200 MPa (116 to 29 ksi) ultra-high-performance-fiber-reinforced concrete. *ACI Material Journal*, 105(6): 603–609.

Lim, J.L.G., Raman, S.N., Hamid, R., Zain, M.F.M., Lai, F.C., 2015 Synthesis of Ultra-High Performance Cementitious Composite incorporating Carbon Nanofibers. In: Proceedings of 6th International Conference on Structural Engineering and Construction Management: pp. 8-13. Kandy, Sri Lanka, Dec. 2015.

Lim, J.L.G., Raman, S.N., Hamid, R., Zain, M.F.M., Lai, F.C., 2018. Synthesis of Nano Cementitious Additives from Agricultural Wastes for the Production of Sustainable Concrete. *Journal of Cleaner Production*, 171: 1150-1160

Metaxa, Z.S., Seo, J.W., Konsta-Gdoutos, M.S., Hersam, M.C., Shah, S.P., 2012. Highly concentrated carbon nanotube admixture for nanofiber reinforced cementitious materials. *Cement and Concrete Composite*, 34(5): 612-617.

Mindess, S., Young, J. F., Darwin, D., 2003. *Concrete*. 2nd Ed. Prentice-Hall, Upper Saddle. United States

Raman, S.N., 2012. New Generation Concrete in Construction: 150 MPa and Beyond. in *In Between: Form + Being* (Edited by M. F. Mohamed & S. N. Raman): pp. 120-123. Faculty of Engineering and Built Environment, UKM, Bangi, Selangor, Malaysia.

Siddique, R., Mehta, A., 2014. Effect of carbon nanofibers on properties of cement mortars. *Construction and Building Materials*, 50: 116-129.

Wille, K., Naaman, A.E., Parra-Montesinos, G.J., 2011. Ultra-high performance concrete with compressive strength exceeding 150 MPa (22 ksi): A Simpler Way. *ACI Material Journal*, 108: 46-54.